10. ELECTRON BEAM LITHOGRAPHY

ZHIPING (JAMES) ZHOU

1. ELECTRON BEAM LITHOGRAPHY AND NANOTECHNOLOGY

The field of nanotechnology covers nanoscale science, engineering, and technology that create functional materials, devices, and systems with novel properties and functions that are achieved through the control of matter, atom by atom, molecule by molecule or at the macromolecular level. The domain of nanoscale structures, typically less than 100 nm in size, lies dimensionally between that of ordinary, macroscopic or mesoscale products and microdevices on the one hand, and single atoms or molecules on the other. There are two approaches to making building block artifacts such as quantum dots, nanotubes and nanofibers, ultrathin films and nanocrystals, nanodevices: bottom-up synthesis and top-down miniaturization.

The bottom-up approach ingeniously controls the building of nanoscale structures. This approach shapes the vital functional structures by building atom by atom and molecule by molecule. Researchers are working to find the mechanism of "self-assembly". "Self-assembly" involves the most basic ingredients of a human body self-reproducing the most basic structures. "Self-assembly" covers the creation of the functional unit by building things using atoms and molecules, growing crystals and creating nanotubes.

"Top down" is an approach that downsizes things from large-scale structures into small-scale structures. For example, vacuum tubes yielded to transistors before giving way to ICs (integrated circuits) and eventually LSIs (large scale integrated circuits). This method of creating things by downsizing from centimeter size to micrometer size is called "microelectronics".

It is a well-known fact that microelectronics has advanced at exponential rates during the past four decades. Due to its rich functionality in applications, low energy consumption in operations, and low cost in fabrication, microelectronics has entered into almost all aspects of our lives through the invention of novel small electronic devices. The most important advancement is the extension of microelectronics and its fabrication methodology into many non-electronic areas such as micro-actuators, micro-jet, micro-sensors, and micro DNA probes.

As this technology continues to advance, it has been extended from micrometer to nanometer scale, hence the existence of "nanotechnology" or "nanofabrication". Using nanotechnology, the narrowest line pattern on massive produced semiconductor devices is now approaching the 50-nanometer level. In research labs, horizontal dimensions of the device feature sizes have been further scaled down from 130 nanometers to 6 nanometers [1] and its vertical dimensions have been reduced to less than 1.5 nanometers or a couple of atoms [2]. These nanoscale devices known as "nanodevices" are obtained through the top-down miniaturization approach.

The heart of the top-down approach of miniaturization processing is the nanolithography technique, such as Electron Beam Lithography (EBL), Nanoimprint Lithography (NIL), X-ray Lithography (XRL), and Extreme Ultraviolet Lithography (EUVL). Among the four techniques of nanolithography, the EBL approach is the front-runner in the quest for ultimate nanostructure due to its ability to precisely focus and control electron beams onto various substrates. It has been demonstrated that electron beams can be focused down to less than 1 nm. This will extend the resolution of EBL to the sub-nanometer region provided that appropriate resistant material is available.

Electron Beam Lithography is a method of fabricating sub-micron and nanoscale features by exposing electrically sensitive surfaces to an electron beam. It utilizes the fact that certain chemicals change their properties when irradiated with electrons just as photographic film changes its properties when irradiated with light. With computer control of the position of the electron beam it is possible to write arbitrary structures onto a surface, thereby allowing the original digital image to be transferred directly to the substrate of interest. EBL followed soon after the development of the scanning electron microscope [3]. Almost from the very beginning, sub-100 nm resolution was reported. As early as 1964, Broers [4] reported 50 nm lines ion milled into metal films using a contamination resist patterned with a 10 nm wide electron beam. Later in 1976, with improved electron optics, 8 nm lines in Au-Pd were reported using a 0.5 nm probe [5]. In 1984, a functioning Aharonov-Bohm interference device was fabricated with EBL [6]. Muray *et al.* [7] reported 1 to 2 nm features in metal halide resists. Until recently, EBL was used almost exclusively for fabricating research and prototype nanoelectronic devices. Currently, its precision and nanolithographic capabilities make it the tool of choice for making masks for other advanced lithography methods.

In EBL nanofabrication, working conditions at which electron scattering causes minimal resist exposure is required. To achieve this goal, either very high energy or very low energy [8] electrons are used. In high-energy case, the beam broadening in the resist through elastic scattering is minimal [5] and the beam penetrates deeply into

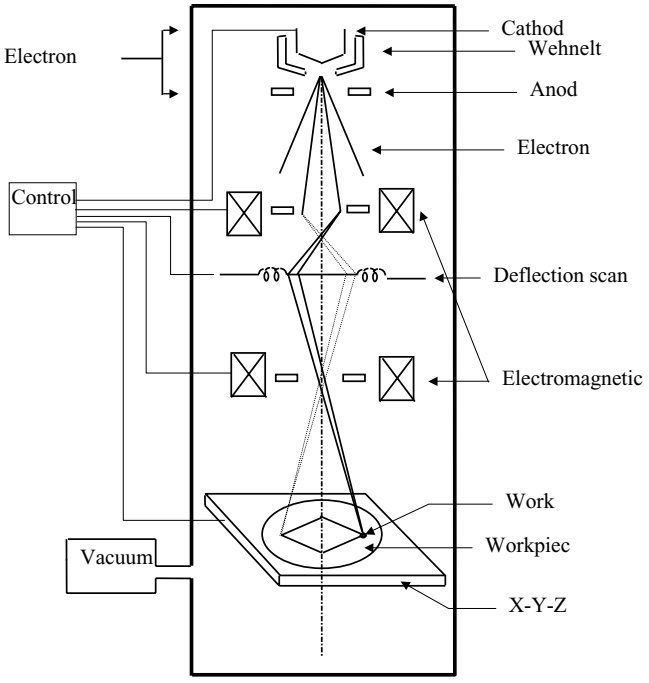

Figure 1. Electron beam lithography instrument. Electrons are generated and accelerated by the electron gun, and guided through the column by the electromagnetic lenses and the deflection scan coil. Both the scanning system and the X-Y-Z stage are used to define the working point on the workpiece.

the substrate. Low energy electron approaches are effective because the electrons have too low an energy to scatter over large distances in the resist.

To implement electronic beam nanolithography into a manufacturing process, speed and precision are required as well as control and yield in the nanofabrication processes. At nanoscale, the fundamental limits of e-beam resist interactions are also important issues, which concern electron scattering and the sensitivity of particular classes of resists to low-voltage in elastically scattered electrons. The issues of throughput, precision, and yield are relevant to instrument design, resist speed, and process control.

2. INSTRUMENTATION OF ELECTRON BEAM LITHOGRAPHY

2.1. Principle

An EBL instrument is a result of working a scanning electron microscope (SEM) in reverse, that is, using it for writing instead of reading. Its view field and throughput are, therefore, limited by the nature of this working principle. Similar as in the SEM, an EBL instrument consists of three essential parts: an electron gun, a vacuum system, and a control system. Figure 1 shows the diagram of an EBL instrument.

An electron gun is a device that generates, accelerates, focuses, and projects a beam of electrons onto a substrate. Electrons are first produced by cathodes or electron emitters. They are then accelerated by electrostatic fields to obtain higher kinetic energy and shaped into an energetic beam. Finally, the guidance system, consisting of the electric and magnetic focusing lenses and deflecting system, transmits the beam to a work point on the substrate.

The electron beam can only be properly generated and unrestrictedly propagated to the substrate in high vacuums. Depending on the material used for the electron gun and the application of the electron beam processing, the vacuum level requirement can usually range from 10^{-3} to 10^{-8} mm Hg. Therefore, the vacuum system, which creates a vacuum environment in the electron gun column and the working chamber, is considered one of the most important parts in the electron beam processing instrument.

The control system provides the manipulation capability for the electron beam generation, propagation, and timing. It also provides control over substrate translation and other functions. The coordination between translating substrates and blinking the electron beam on and off makes it possible to transfer the AutoCAD design onto a thin layer of electron beam resist.

There are two ways to generate actual patterns using an EBL instrument: raster-scanning and vector-scanning. A raster-scanning system patterns a substrate by scanning the exposing beam in one direction at a fixed rate while the substrate is moved under the beam by a controlled stage. In order to compose a designed pattern the electron beam is blanked on and off thousands of times during each scan. It is much like the raster scanning of a television. The vector-scanning scheme attempts to improve throughput by deflecting the exposure beam only to those regions of the substrate that require exposure. In this way, significant time can be saved since the beam skips over the areas that have no pattern.

2.2. Electron Optics

The theory of electron beam lithography can be understood through the electron motion in electric and magnetic fields and the basic Electron Optical Elements. Generally speaking, the electron motion in electric and magnetic fields can be described by Maxwell's equations. However, it is very difficult to solve the practical design problem of an electron beam system by simply applying the boundary conditions to the Maxwell's equations. Therefore, only the basic electron dynamics will be given in this section.

2.2.1. Basic Electron Dynamics

Assuming the velocity of the electrons during the processing is very small compared to the speed of light, assuming the applied electric and magnetic fields are static or varying slowly so that they can be treated as constants, and assuming electrode shapes, potentials, and magnetic field configuration are known, the general equation of motion

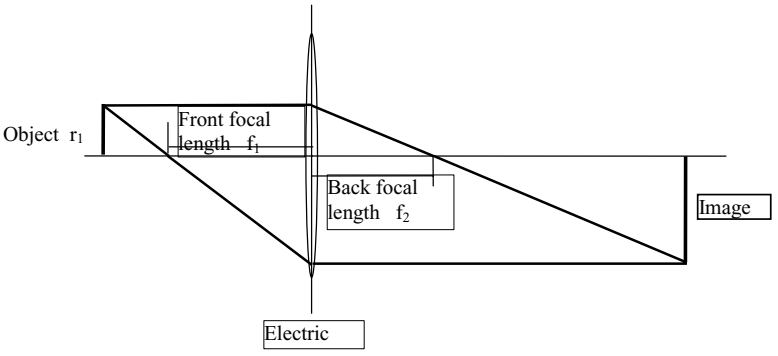

Figure 2. Ray diagram of electric lens. It is used for deriving the focal lengths of a thin lens.

for an electron in electric and magnetic fields can be written as:

$$\frac{d^2\mathbf{r}}{dt^2} = \frac{q}{m}(\mathbf{E} + \mathbf{v} \times \mathbf{B}) \tag{1}$$

where q is the charge of the electron, m the mass of the electrons, and $\mathbf{r}$ a position vector locating the electron with respect to any origin. $\mathbf{E}$ and $\mathbf{B}$ denote electric and magnetic field, respectively. $\mathbf{v}$ is the velocity of the electron moving in the fields.

ELECTRIC LENS Considering an axially symmetric field system of the electron beam generating column, the electron beam passes through a common point near the axis can be made to pass through another common point by a relatively limited region of the field variation. In analogy to the light optics, it is appropriate to call the first common point the object, the second the image, and the region of the fields the electric lens. Properties and parameters of the electric lens can be derived from the following paraxial ray equation:

$$\frac{d^2r}{dz^2} + \frac{dr}{dz}\left(\frac{V_0'}{2V_0}\right) + \frac{r}{4}\frac{V_0''}{V_0} = 0 \tag{2}$$

where V_0 is the potential on the axis. For examples, since the derivatives V_0' and V_0'' are normalized with respect to V_0, it is understandable that the field distribution rather than the intensity of the potential will determine the electron trajectories. The equation is unchanged in form even if a scale factor is applied to the location r. This indicates that all trajectories parallel to the axis will have the same focus regardless of their initial radius. It should be noticed that the electron charge q and electron mass m are absent from the ray equation. This implies that the equation is also applicable to other particles such as ions. Using the ray diagram in Figure 2, two focal lengths of a thin electric

lens can be obtained from equation (2) as

$$\frac{1}{f_i} = (-1)^i \frac{1}{4\sqrt{V_i}} \int_1^2 \frac{V_0''}{\sqrt{V_0}}\, dz \quad i = 1, 2 \tag{3}$$

and the relationship between two focal lengths is similar to that in optics

$$\frac{f_2}{f_1} = -\frac{\sqrt{V_2}}{\sqrt{V_1}}, \tag{4}$$

where $\sqrt{V_i}$ is equivalent to the optical index of refraction, N_i.

Magnetic lens As in the electric case, an axially symmetric magnetic field also has lens characteristics and is called a magnetic lens. The paraxial ray equation for a magnetic lens is written as:

$$\frac{d^2r}{dz^2} = \frac{\frac{q}{m} r\, B_0^2}{8V} \tag{5}$$

where B_0 is the magnetic field on the axis. Clearly, the magnetic lens effect will depend on the charge and mass of the electrons involved. The magnetic lens is symmetrical because the equation is unchanged if B_0 is reversed in sign. The spatial invariance of the magnetic lens ensures that electronic imaging can be performed without distortion near the axis. Similar to the case of the electric lens, the focal lengths are given as

$$\frac{1}{f_2} = -\frac{\frac{q}{m}}{8V} \int_1^2 B_0^2\, dz \tag{6}$$

and

$$f_1 = -f_2. \tag{7}$$

The symmetry in equation (5) has been applied to obtain the equation (7). Since electrons have a negative charge of q, the back focal length of f_2 is always positive. Therefore, the magnetic lens is always convex.

Bipole element Electron beam deflection could be achieved by using electrostatic and magnetic bipole elements. An electrostatic field will bend the passing electron beam towards the positive pole, while a magnetic field deflects the beam to the direction perpendicularly to the direction of the field. A pure magnetic field will change the direction of the electron's motion, but not the speed. The relationship between the

magnetic field and the curvature of the electron path can be written as

$$R = \frac{mv}{qB\sin\theta} \tag{8}$$

where R is the instantaneous center of curvature and θ is the angle between the magnetic field and the velocity vectors.

Equations (1)–(8) describe the focusing imaging, and deflection of the electron beam and provide the basic electron dynamics needed in simple electron beam system design.

2.2.2. Electron Optical Elements

Compared with other lithography instrument, the use of electron guns is the core characteristic of the electron beam lithography technique. The principles of electron guns can be understood through the way of optical pass to rays of light. The electron optical elements are simply their optical counterparts. Therefore, this section will be mainly focused on the electron guns, including source generation, beam shaping, and the beam guiding system.

Based on the physical laws of electron emission and the desired energy conversion at the work point, almost all guns are of similar design, although they might differ widely with respect to beam power, acceleration voltage, and electron current. In the gun, free electrons are first generated from emitters, or cathodes, and are then shaped into a well-defined beam, which is ultimately projected onto the work point. The common concerns of the source generation and beam shaping systems are described below.

Source generation

Emission There are two kinds of electron emission. The first kind, called thermionic emission, happens when the emissive materials are heated up to a high enough temperature. The second type is field emission, in which electrons are produced due to an intense applied electric field. Since thermionic emission has higher efficiency in producing electrons at lower cost, it is widely used in industry and will be our primary concern here.

According to quantum dynamics, electrons are at rest in the ground state at 0°K and their energy levels and bands are well defined. As the temperature of the material increases, some electrons obtain more energy and jump to higher energy levels. Therefore the width of the energy bands increases. When the temperature is high enough, the electrons obtain sufficient energy to overcome the natural barrier, the work function that prevents them from escaping. In particular, as the temperature increases, the upper limit on the conduction band of metals smears and stretches out. Some of the conduction electrons obtain enough energy to overcome the potential barrier at the surface of the metal. These electrons may then be drawn off by the application of a suitable field. If the field is sufficiently high to draw all the available electrons from a cathode of work function Φ, the saturation current density J obtained at temperature T

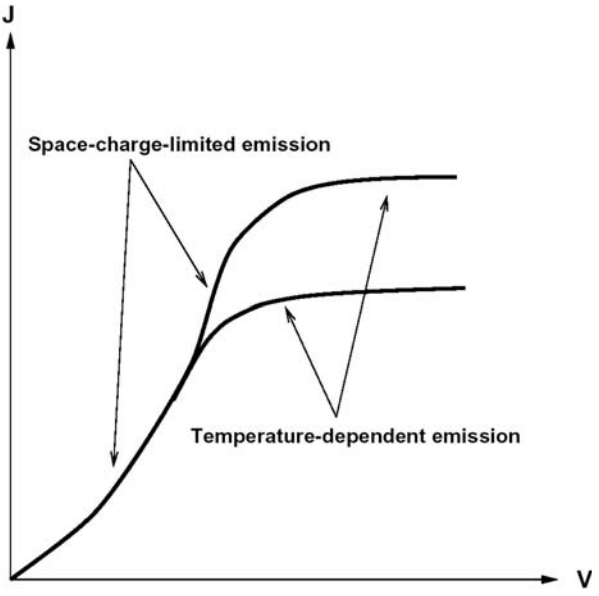

Figure 3. Space-charge-limited emission and temperature-dependent emission. Most cathodes in electron guns operate in the transition range between the space-charge and saturation regimes so that the desired emission current density can be obtained at the lowest cathode temperature.

is given by the well-known Richardson-Dushman Law

$$J = AT^2 \exp\left(-\frac{q\Phi}{kT}\right) \tag{9}$$

where A is a constant determined by the material and k is the Boltzmann constant.

In practical electron gun design, less than the saturation current is usually drawn from the gun. In this situation, the field is not strong enough to draw off all the available free electrons from the cathode. Therefore, the residual electrons are accumulated near the surface of the cathode, forming an electron cloud layer. Such operation, termed space-charge-limited emission, has the advantage that a smaller virtual cathode is formed slightly in front of the cathode that has a stable charge density, essentially independent of cathode temperature. The current that flows between parallel electrodes is given by Child's law [9]

$$J = \frac{4\sqrt{2}\varepsilon_0}{9}\sqrt{e/m}\frac{V^{3/2}}{L^2} = 0.0233\frac{V^{3/2}}{L^2} \tag{10}$$

where V is the acceleration voltage and L is the distance between the cathode and anode.

Figure 3 shows the current density in the range of space-charge-limited emission and temperature-dependent emission. Most cathodes in electron guns operate in the

transition range between the space-charge and saturation regimes so that the desired emission current density can be obtained at the lowest cathode temperature.

Equations (9) and (10) give the conditions for obtaining the required emission from a given cathode material. As long as the material is specified, the preliminary cathode design can be completed.

Materials Free electrons may be obtained from the cathodes of many kinds of materials. However, the primary gun design requirements are that the cathode has a low work function and good thermal efficiency, supplies an adequate emission current, and is simple to construct. Among all the constraints, the vacuum condition of the electron gun puts strong limits on the choice of cathode materials.

At low vacuum level (less than 1×10^{-5} mm Hg), materials with low work functions and high bulk evaporation rates, such as barium, are frequently used. The material is first contained within the body of another material which provides structure and shape for the cathode, and then migrated to the surface by a diffusion process. This kind of cathode is called a dispenser cathode. The dispenser cathode generates and maintains an excess of barium metal at its surface and relies on that excess for its emission properties. In this configuration, the evaporation of the materials can be slowed down and easily controlled.

At vacuum levels higher than 1×10^{-5} mm Hg, the choice of cathode material is restricted to the refractory metals, which have higher work functions and operate at higher temperatures. The most attractive refractory metals are tungsten and tantalum with work functions of 4.55 and 4.1 electron volts, respectively. The melting point of tungsten is 3410°C, while that of tantalum is 2996°C. At temperatures below 2500°C, tantalum will emit 10 times the current of tungsten. Tantalum is also easy to work with and can be formed into a sheet to produce special cathode shapes.

If the vacuum is to be recycled to atmosphere but not operated above 5×10^{-6} mm Hg, a cathode of lanthanum hexaboride (LaB_6), with work function of 2.4 electron volts, may be used [10]. This arises from the need for relatively high emission current densities at lower emission temperatures. Among other activated cathodes, LaB_6 is much less sensitive to problems such as cathode contamination and lifetime but its long-time stability and thermal cycling stability are still unsolved problems.

Among all these cathode materials, tungsten may not be the best in most respects, but for normal applications it is a cheap, robust, and reliable emissive source. As of today, tungsten remains the most important cathode material in the field of electron beam processing, even though tantalum, LaB_6, as well as tungsten with emission-increasing alloying elements are also widely used.

Beam shaping and guidance After the free electrons are emitted from the cathode, they are first shaped into a well-defined beam with the desired beam diameter and focal length and then guided to the work point on the workpiece. This is achieved through different gun design and via focusing and deflection by using the principles of electron optics.

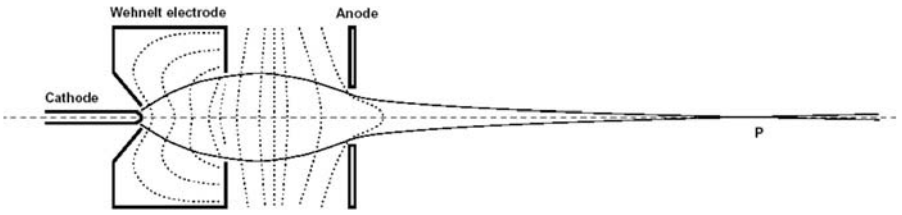

Figure 4. Three-electrode telefocus gun. Its long focal length is primarily due to the hollow shape and negative bias of the Wehnelt electrode, which acts as a simple electrostatic lens.

Gun type A basic electron gun consists of a cathode, a focusing electrode, and an anode. It is called a two-electrode gun if the focusing electrode has the same potential as that of the cathode. A design with different potentials of the cathode and the focusing electrode is called a three-electrode gun. Multielectrode guns have several focusing electrodes or control electrodes at different potentials.

Analogous to the terminology in light optics, it is called an axial gun if the elements of the beam-generating system, the electrostatic field, and the beam itself are rotationally symmetrical. There are three basic axial gun types for general use: the Telefocus gun, the Gradient gun and the Pierce gun.

The Telefocus gun is a three-electrode gun, see Figure 4. It is primarily designed to produce a relatively long focal length. The long focus effect is due to the hollow shape and negative bias of the Wehnelt electrode, which acts as a simple electrostatic lens. It operates as follows. First, the electrons near the cathode are pushed outwards along the diverging electric field. Due to the special design, the equipotentials between the Wehnelt electrode and the anode then become flat, and finally converge toward the anode (shown as dotted lines). At this final step, the electron beam obtains a net radial velocity inward. The magnitude of the net radial inward velocity is smaller than the initial outward velocity because the electrons now have higher energy. Consequently the electron beam converges quite slowly and has a long focal length. If the bias on the Wehnelt electrode increases, the field curvature in the cathode region also increases. Therefore, the focal length will be longer because the starting electron beam is more divergent. The ray traces are shown in solid lines. Position P is the focal point.

The Gradient gun [11] shown in Figure 5 is a post-acceleration gun. Similar to the conventional triode, the relatively high voltages and large currents are controlled by a small "grid" voltage V_1. Thus the total beam power may be varied over a wide range with a small variation in spot size. In order to take full advantage of the gun's capabilities, the total accelerating voltage must be much larger than the controlling voltage V_1. Also, V_1 must be high enough to draw adequate emission from the cathode.

In many applications in semiconductor manufacturing, uniform high intensity electron beams are required. It was suggested by Pierce that such a uniform electron beam could be obtained over a limited region if the region is considered a segment of extensive beam flow, and the electrodes, including cathode and anode, are shaped to maintain

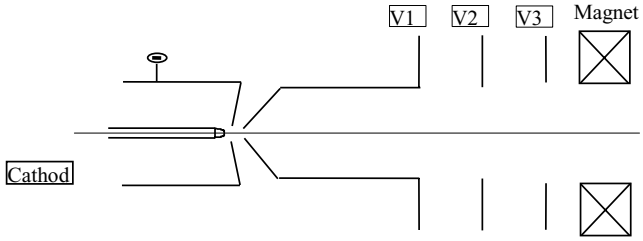

Figure 5. Triode gradient gun. Similar to the conventional triode, the relatively high voltages and large currents are controlled by a small "grid" voltage V_1. Thus the total beam power may be varied over a wide range with a small variation in spot size.

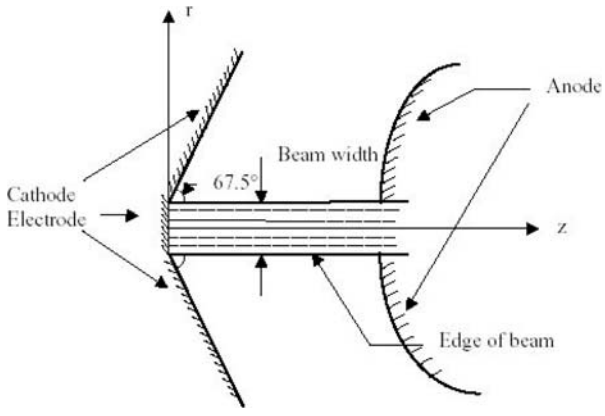

Figure 6. Two-electrode pierce gun. It is designed to produce, under the space-charge-limited emission, a parallel or slightly divergent uniform high intensity electron beams.

the same voltage along the edge of the segment. The so-called Pierce gun is designed to produce, under the space-charge-limited emission, a parallel or slightly divergent beam, see Figure 6. In this design, a broad electron beam is emitted by a flat cathode and propagates as a parallel laminar flow with a sharp planar or cylindrical surface. To keep this beam propagating as a parallel beam, the shape of the electrodes outside the beam must be carefully considered. The simplest solution is to have a 67.5° angle at the cathode and the curved anode surface, which coincides with an equipotential. A spherically curved cathode will converge the beam. However, the resultant focus point will be relatively large due to the outward directed force of the space charge. The Pierce gun is a two-electrode gun and is easy to design. The beam can be parallel, divergent or convergent. The efficiency of the gun can be as high as 99.9 % or more.

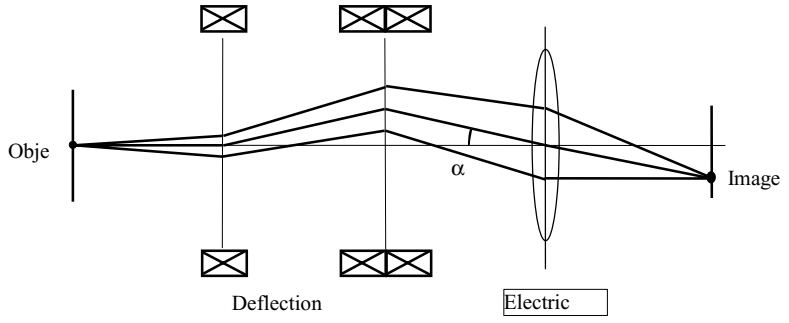

Figure 7. A double deflection system in which a focal point at the object plane is deflected by α degree at the image plane.

Beam guidance Shaped in the gun, the beam is characterized by the parameters of the focal spot. The most important focal spot parameters are the diameter and location of the focal spot on the axis, the current density and current density distribution on the focal plan, and the aperture. The object of the beam guidance system is to transform these parameters into parameters required by the particular application process on the workpiece. Figure 7 shows a simple beam guiding system. In this system, a focal point at the object plane is first deflected by a double deflection system, and then imaged and refocused onto the image plane. For some applications, the beam diameter formed inside the gun must be imaged either on an enlarged or reduced scale to obtain a beam with a defined diameter, a particular current density, and a specified power density on the workpiece. The beam current at the working point may be lower than the beam current in the gun through aperture limiting. Other applications may require that the beam be guided into the working chamber without any noticeable loss in beam current.

Like all other electron beam applications, beam guidance for electron beam processing is achieved via imaging, focusing and deflection under the principles of electron optics. In general, rotationally symmetrical magnetic fields produced by magnetic-lens systems are used for imaging and focusing; either plain or crossed magnetic bipole elements are often used for beam deflection. In the case of turning the beam over wide angles, magnetic sector fields may be added for additional deflection.

The magnetic lenses can be generated by permanent magnets. It can also be created by electrical coils. The simplest magnetic lenses are iron-clad coils, as shown in Figure 8. In this configuration, the magnetic induction is proportional to the excitation NI, where N is the number of turns and I is the coil current. The magnetic field profile and the electron optical features of the lens are totally dependent on the gap width, w, and the bore diameter of the pole pieces, D. In practice, the aberration and astigmatism should also be considered in lens design.

It can be seen from Equations (6) and (7) that all magnetic lenses are convex lenses. These lenses can be used for either producing a magnified image of the object or

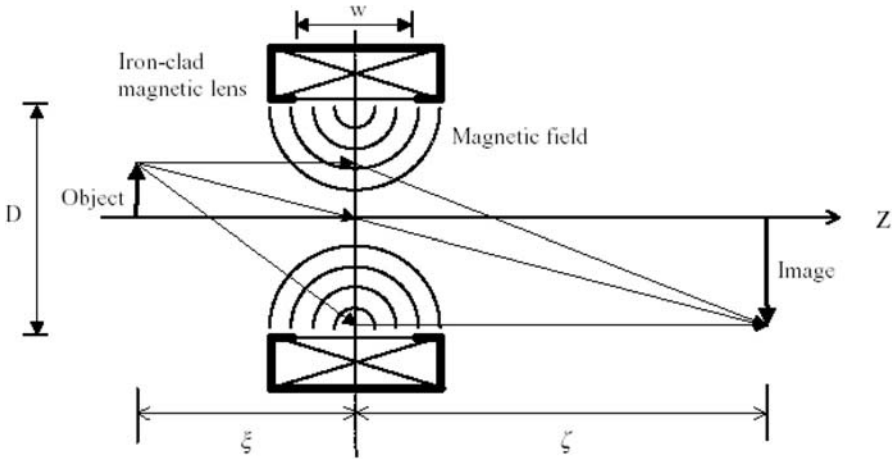

Figure 8. A magnetic lens generated by iron-clad coils, which is a basic element of the electron beam processing equipment to project an electron beam pattern to the workpiece.

focusing a parallel electron beam to a fine point. Assuming the front and back focal lengths of the convex "thin" lens are same, Newton's lens equation can be applied for the electron beam formation:

$$\frac{1}{\xi} + \frac{1}{\zeta} = \frac{1}{f} \tag{11}$$

where u is the distance between the object and the lens, v the distance from the lens to the image, and f the focal length of the lens. It can be seen that to obtain a real magnified image, both ξ and ζ should be greater than f. The magnification is defined as:

$$M = \frac{\zeta}{\xi}. \tag{12}$$

As in a well-designed optical imaging system, it is often necessary to change the magnification while operating the electron beam system. The magnification of the electron beam system is varied by changing the strength of its electric or magnetic lens. This is totally different from the light beam system, in which the magnification is changed by moving the optical lens or the objective back and forth.

Both electrostatic and magnetic bipole elements can be used for beam turning and deflection. They are created by electrical fields between two plates or by magnetic fields between the opposite poles of a permanent magnet and inside current-carrying coils. In electron beam processing, the electrostatic bipole element is usually employed for beam blanking or some other special purposes.

There are many designs of magnetic bipole elements. In the simplest case, the field between the poles of a permanent magnet is used for deflection. The pole-piece spacing w and their width b are usually much larger than the electron beam diameter. In most of cases, the magnetic fields for deflection elements are produced electromagnetically. The magnetic induction B is directly proportional to the excitation NI, and indirectly proportional to the pole-piece spacing w. In order to obtain the highest possible induction at a given excitation, the magnetic circuit must have fairly large dimensions.

Figure 9(a) and (b) shows narrow and wide angle deflection in a uniform magnetic field normal to the electron beam direction. Based on electron dynamics, the radius of the electron trajectory is given by

$$R = \left(\frac{2m}{q}\right)^{1/2} \frac{V^{1/2}}{B} = 3.37 \times 10^{-6} \frac{V^{1/2}}{B}. \tag{13}$$

When the electron beam vertically enters a limited magnetic field [12], the beam deflection over a narrow angle is expressed as:

$$\sin\theta = 2.97 \times 10^{5} \frac{LB}{V^{1/2}} \tag{14}$$

where L is the field length. In a magnetic sector field, the deflection angle can be found through the following equation:

$$\theta = \alpha - \beta_1 + \beta_2 \tag{15}$$

Clearly, the deflection angle can be enlarged by increasing the sector angle α.

3. ELECTRON-SOLID INTERACTIONS

3.1. Electron Scattering in Solid

As the electrons penetrate the solid materials, such as the electron beam resist, the interaction can be characterized by scatterings. There are two kinds of scatterings during the electron-solid interaction: small angle scattering (forward scattering), which tends to broaden the initial beam diameter, and the large angle scattering (backscattering), which causes the proximity effect [13], where the dose that a pattern feature receives is affected by electrons scattering from other nearby features. The backscattering happens as the electrons penetrate through the resist into the substrate.

During the interaction, the primary electrons slow down, producing a cascade of electrons called secondary electrons with energies from 2 to 50 eV. These are responsible

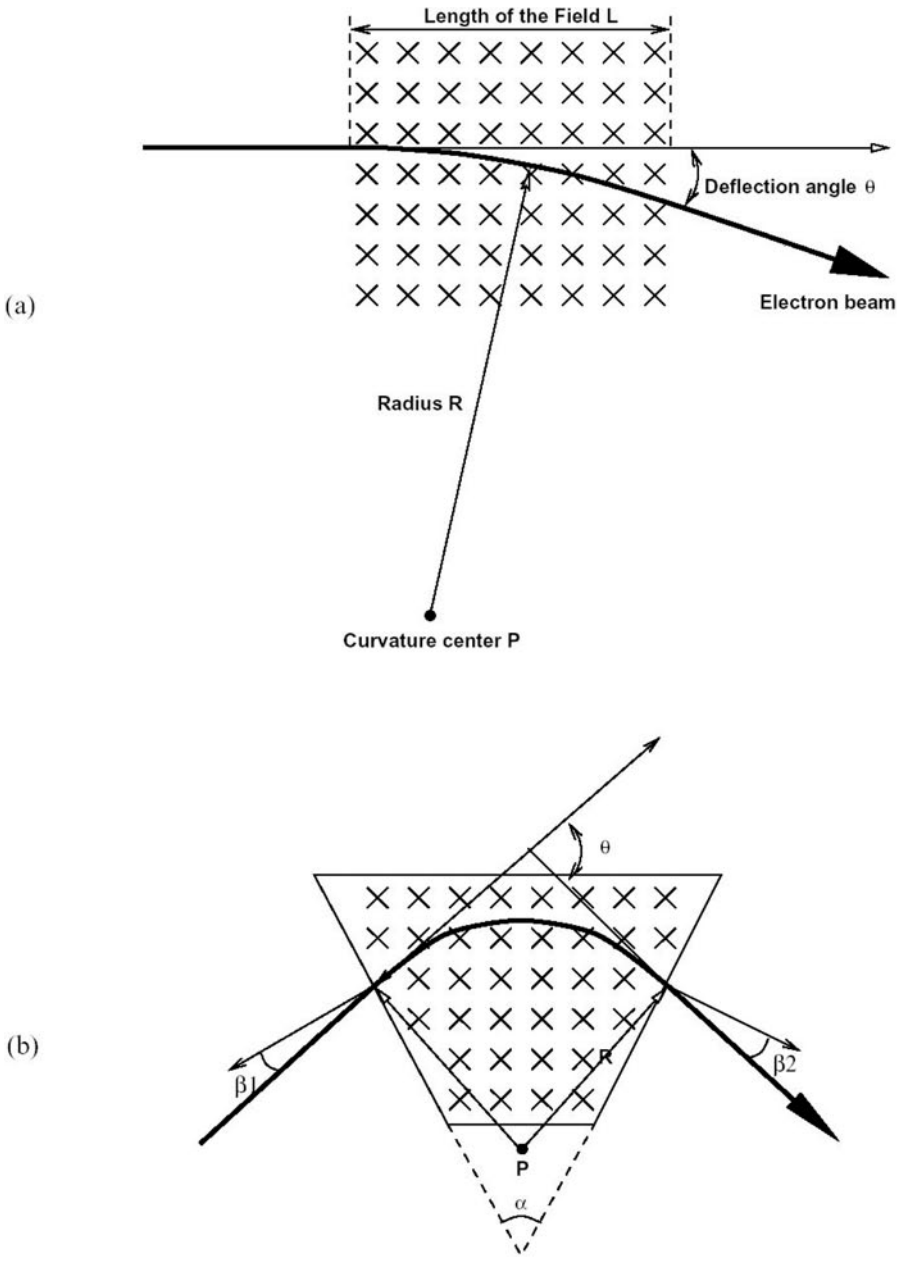

Figure 9. Electron beam deflection in a homogeneous magnetic field: (a) deflection in a limited field; (b) bending in a sector field. The sector field produces larger deflection angle.

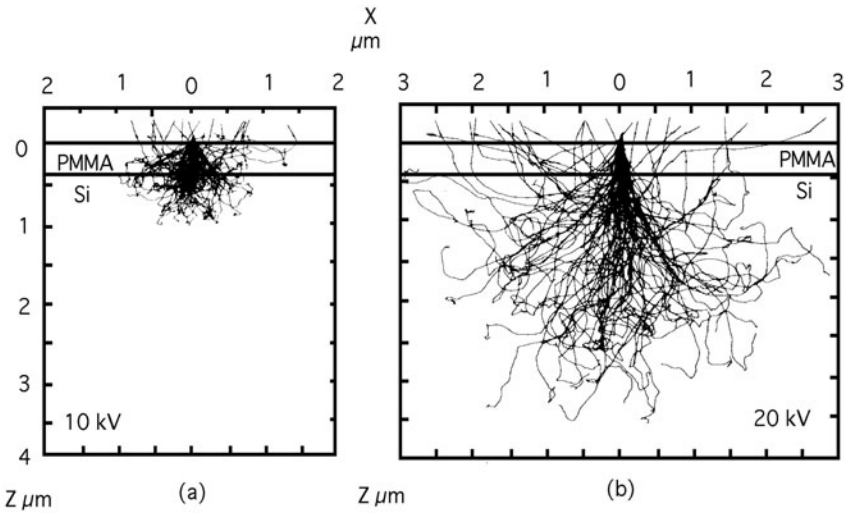

Figure 10. Monte Carlo simulation of electron scattering in resist on a silicon substrate at a) 10 kV and b) 20 kV (Kyser and Viswanathan, 1975).

for the bulk of the actual resist exposure process. Since their range in resist is only a few nanometers, they contribute little to the proximity effect. However, a small fraction of secondary electrons may have significant energies, on the order of 1 keV. These so-called "fast electrons" can contribute to the proximity effect in the range of a few tenths of a micron.

Figure 10 shows a computer simulation of electron scattering in typical samples [14]. The combination of forward and backscattered electrons results in an energy deposition profile in the resist that is typically modeled as a sum of two Gaussian distributions.

3.2. Proximity Effect

The result of the electron scattering is that the dose delivered by the EBL system is not confined to the shapes that the system writes. This results in pattern specific linewidth variations known as the proximity effect. Due to the proximity effect, a narrow line between two large exposed areas may receive so many scattered electrons that it can actually be developed away in positive resist.

Higher beam voltages, from 50 kV to 100 kV, are used to minimize both forward and backward scatterings when writing on very thin membranes such as those used for x-ray masks [15]. On the other hand, by using very low beam energies, where the electron range is smaller than the minimum feature size, the proximity effect can also be eliminated [8]. In this case, the thickness of a single layer resist must also be less than the minimum feature size so that the electrons can expose the entire film thickness.

3.3. Electron Beam Resists

EBL is classified as a reactive processing in terms of Electron Beam Processing. In this process, ionization and excitation of constituent molecules of the material occur during the scattering of the incident electrons. Some excited molecules lose their energy by collisions with other molecules and change into radicals. All these ions, excited molecules, radicals, and the secondary electrons are called active species that induce chemical reactions inside the material. Electron beam resists are used as the recording and transfer media for EBL process. The electron beam exposure alters the nature of the resist, through the breaking of chemical bonds, with the result that a subsequent immersion of the sample in a chemical solution removes the exposed parts, or the unexposed parts, of the resist film.

Therefore, the selected resist must be sensitive to the active species, which means that it must be altered by the beam in such a way that, after development, the portions exposed to the beam are removed (positive resist), or remain (negative resist). These materials are usually polymeric solutions that are applied to the surface of the substrate by a spin coater and dried by baking to form a uniform thin layer. To reduce proximity effects, positive resist is usually exposed and/or developed lightly while still adequately clearing the resist down to the substrate for all features.

In the EBL process, it is possible to make resist structures with very high aspect ratios (>5:1). But, when the aspect ratio exceeds about 5:1, the tall features may fall over during development, due primarily to surface tension in the rinse portion of the development sequence. For typical applications, the resist thickness should not exceed the minimum feature size required.

When exposing resist on insulating substrates, substrate charging causes considerable distortion [16]. A simple solution for exposure at higher energies (>10 kV) is to evaporate a thin (10 nm) layer of gold or chrome on top of the resist. Electrons travel through the metal with minimal scatter, exposing the resist. The metal film should be removed before developing the resist [17–18].

3.3.1. PMMA Electron Beam Resists

Polymethyl methacrylate (PMMA) is the standard high-resolution polymeric electron beam resist. PMMA at lower doses is a positive-acting resist and at higher doses is a negative-acting resist. For line doses the sensitivity difference between the positive resist and the negative resist is a factor of 20–30X. The best resolution obtained in PMMA was 10-nm lines in its positive mode. In negative mode, the resolution is about 50 nm. It was suggested [19] that the limitation was due to secondary electrons generated in the resist, although the effect of molecule size and development could also play a role. By exposing PMMA on a thin membrane, the exposure due to secondary electrons can be greatly reduced and the process latitude thereby increased.

The sensitivity of PMMA is roughly proportional with electron acceleration voltage, with the critical dose at 50 kV being roughly twice that of exposures at 25 kV. When using 50 kV electrons and 1:3 MIBK:IPA developer, the critical dose is around 350 $\mu C/cm^2$. PMMA has poor selectivity in plasma etching, compared to

novolac-based photoresists. It has an approximately 1:1 etch selectivity for silicon nitride [20] and silicon dioxide [21]. PMMA makes a very effective mask for chemically assisted ion beam etching of GaAs and AlGaAs [22].

3.3.2. Positive Resists

In positive resists, electron beam breaks polymer backbone bonds and transfer the exposed polymer into fragments of lower molecular weight. A solvent developer selectively washes away the lower molecular weight fragments and leaves the unexposed portion of the resist film intact. Three most commonly used positive resists are described below.

EBR-9 EBR-9 is an acrylate-based resist, poly(2, 2, 2-trifluoroethyl-chloroacrylate) [23]. It is 10 times faster than PMMA. But, its resolution is more than 10 times worse than that of PMMA. EBR-9 is perfect for mask-writing applications, not because of its speed but because of its long shelf life, lack of swelling in developer, and large process latitude.

PBS Poly(butene-1-sulfone) (PBS) is a common high-speed positive resist used for mask making due to its very high sensitivity ($\sim$1 to 2 $\mu C/cm^2$). However, the processing of PBS is difficult: masks must be spray developed at a tightly controlled temperature and humidity [24]. For small to medium scale mask production, the time required for mask processing can make PBS slower than some photoresists [25].

ZEP ZEP-520 from Nippon Zeon Co. [26] is a relative new resist for EBL. It consists of a copolymer of -chloromethacrylate and -methylstyrene, with sensitivity of an order of magnitude faster than PMMA and similar to the speed of EBR-9. Comparing with EBR-9, the resolution of ZEP is very high and close to that of PMMA. ZEP has about the same contrast as PMMA. The etch resistance of ZEP in CF_4 RIE is around 2.5 times better than that of PMMA but is still less than that of novolac-based photoresists.

3.3.3. Negative Resists

In negative resists, electron beam cross-links the polymer chains together so that they are less soluble in the developer. Negative resists have less bias (the difference between a hole in the resist and the actual electron beam size) than positive resists. However, they tend to have the problems of insoluble residue in exposed areas, swelling during development, and bridging between features. Two commercially available negative electron beam resist are follows.

COP COP is an epoxy copolymer of glycidyl methacrylate and ethyl acrylate, P(GMA-co-EA). The speed of this resist is very high: 0.3 $\mu C/cm^2$ at 10 kV. But the resolution is only about 1 um [27]. The plasma etch resistance of COP

is relatively poor. The resist requires spray development to avoid swelling. Because cross-linking occurs by cationic initiation and chain reaction, the cross-linking continues after exposure. Therefore, the size of the features depends on the time between exposure and development. COP is commonly used for making mask plates [28–29].

SAL The popular SAL resist [30] consists of three components: a base polymer, an acid generator, and a crosslinking agent. After exposure, a baking cycle enhances reaction and diffusion of the acid catalyst, leading to resist hardening by cross-linking. Common alkaline photoresist developers will dissolve the unexposed regions. The acid reaction and diffusion processes are important factors in determining the resolution [31], and a tightly controlled postexposure baking process is required. The extent of the cross-linking reaction is therefore affected by the thermal conductivity of the sample and by the cooling rate after the bake. The sensitivity of SAL is about 7 to 9 $\mu C/cm^2$ at either 20 or 40 kV, and is therefore suitable for mask making. A resolution of 30 nm has been demonstrated at very low voltage [32], and 50 nm wide lines have been fabricated using high voltage [33]. This novolac base polymer has etching properties similar to those of positive photoresists. It is interesting to note that, unlike PMMA, the critical dose of SAL does not scale proportionately with accelerating voltage. Although it is not as sensitive as other negative resists, such as COP, SAL has far better process latitude and resolution.

3.3.4. Multilayer Systems

Multilayer resist systems are needed in the following cases: when an enhanced undercut is needed for lifting off metal, when rough surface structure requires planarization, and when a thin imaging (top) layer is needed for high resolution.

Bilayer systems The simplest bilayer technique is to spin a high molecular weight PMMA on top of a low molecular weight PMMA. The low weight PMMA is more sensitive than the top layer, so the resist develops with an enhanced undercut. The two-layer PMMA technique was patented in 1976 by Moreau and Ting [34] and was later improved by Mackie and Beaumont [35] by the use of a weak solvent (xylene) for the top layer of PMMA.

Trilayer systems Virtually any two polymers can be combined in a trilayer resist if a barrier such as Ti, SiO_2, aluminum, or germanium separates them [36–37]. This trilayer system has been applied for fabricating dense and high aspect ratio resist profiles as described below. First, the top layer is exposed and developed and the pattern is transferred to the interlayer by RIE in CF_4 (or by Cl_2 in the case of aluminum). Then, using the interlayer which serves as an excellent mask, the straight etch profile is obtained by oxygen RIE. Such high aspect ratio of resist profiles can then be used

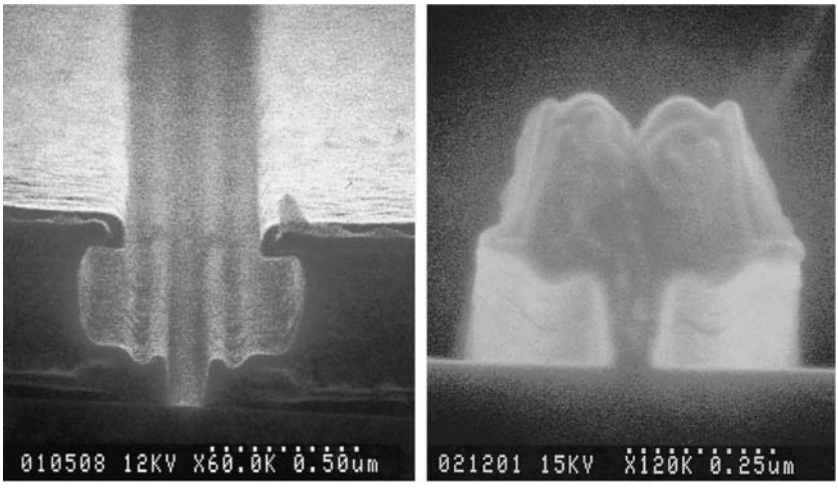

Figure 11. (a) Resist cross-section (PMMA on P(MMA-MAA) on PMMA) for the lift-off of a "T" shaped gate. (b) Metal gate lifted off on GaAs (R. C. Tiberio *et al.*, 1989).

for liftoff or for further etching into the substrate. Figure 11 shows two gate structures obtained by using the multiplayer system [38].

4. PATTERN TRANSFER PROCESS

After the resist is patterned by EBL, it is necessary to transfer the pattern onto the underlying substrate. There are two basic pattern transfer methods: additive process or subtractive process.

4.1. Additive Processes

Lift-Off and Plating are two basic additive processes as shown in Figure 12 and Figure 14.

4.1.1. Lift-Off Process

The lift-off process is based on the following requirements: there is an undercut profile in developed resist and the resist remains soluble after other material has been deposited onto it. The undercut profile is used as a "stencil" during the additive deposition process. Since the resist remains soluble after the deposition, soaking the substrate in a good resist solvent lifts the unwanted material together with the resist while the desired pattern structure remains on the substrate, hence the name "Lift-off", (see figure 12). It was predicted and observed that undercut profiles can be obtained in PMMA resist under a certain exposure dose and beam voltage [39–40]. Figure 13 shows that about

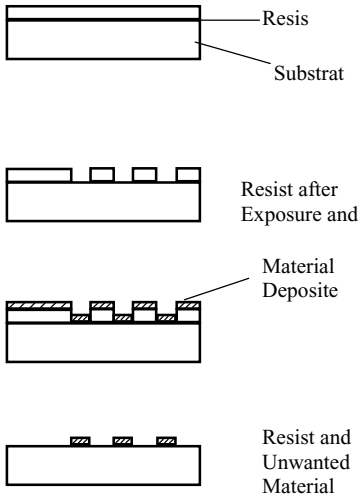

Figure 12. The lift-off process flow.

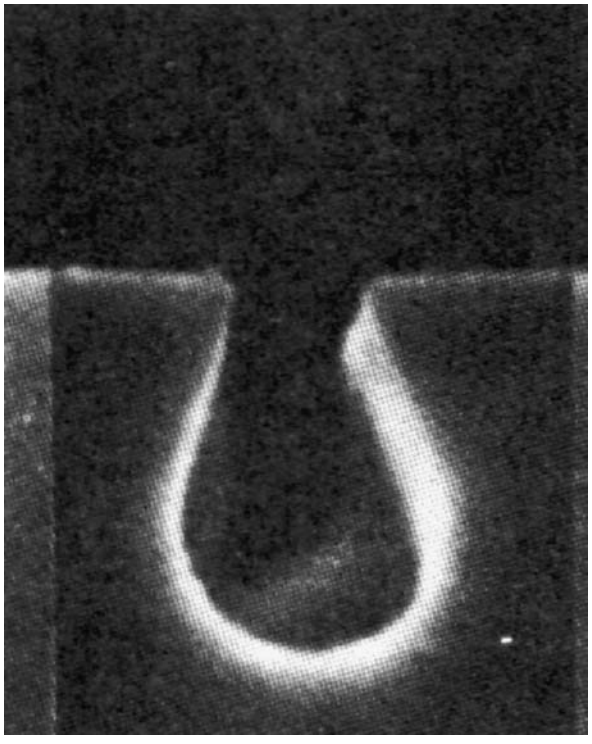

Figure 13. An undercut profile in PMMA resist.

100 $\mu C/cm^2$ at 15 kV produces a good undercut profiles in one micron thick PMMA resist.

In order to apply lift-off successfully, however, certain requirements must be met. 1). The resist undercut profile angle to the surface normal must always be larger than the deposition beam angle. 2). The temperature stability of the resist, which is determined by the glass transition temperature, Tg, should not be exceeded during the material deposition or substrate cleaning. Above Tg, the resist will flow and cause distortion of developed image and loss of the undercut profile. For PMMA resist, it will flow above 110°, therefore, care should be taken not to exceed 100°C temperature on the substrate during deposition. 3). Care also should be taken to remove the resist and clean the substrate after the material deposition. 4). The resist should remain soluble in some solvent or liquid after deposition, otherwise, lift-off cannot be completed. In some cases, ultrasonic agitation may be necessary in order to lift-off the unwanted metal, although this should be used only as a last resort, since the deposited pattern on the substrate may also be damaged especially if the material adhesion to the substrate is not very good.

4.1.2. Plating Processes

The second additive technique, which has found uses in circuit board fabrication and also in nanofabrication of such devices as zone plates for x-ray imaging, is plating of the metal in the areas where the resist has been removed after development. More recently this technique has also been used in the fabrication of x-ray masks where gold is used as the absorber. The most commonly used method is electroplating and this requires that a thin, electrically conducting layer is used as a plating base under the resist that is continuous over the entire surface of the substrate so that electrical contact can be made to it during electroplating. Figure 14 shows a schematic of the plating process.

4.2. Subtractive Processes

Subtractive patterning processes comprise all processes in which the layer to be patterned is deposited first, as a uniform layer, on the substrate followed by the resist, Figure 15. After exposure and development, the parts of the underlayer not protected by the resist, are removed either by immersion in an acid or other liquid, (wet etching), or by placement in a plasma reactor in which a chemically active gas has been added, (dry etching). Although wet etching is very fast and inexpensive, this process presents a major disadvantage that prohibits its use in high-resolution lithography. The resolution limitation of wet etching is a direct result of undercutting or metal etching under the resist mask due to the isotropic nature. Subtractive patterning in micro and nanostructure fabrication became possible only after the development of plasma or dry etching and specifically reactive ion etching, (RIE) in which the reactive gas ions are accelerated on to the surface of the resist covered substrate striking it

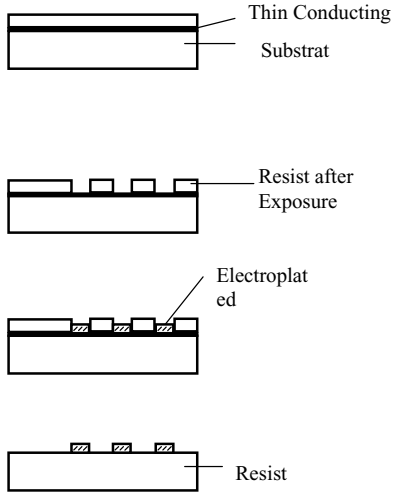

Figure 14. The electroplating process flow.

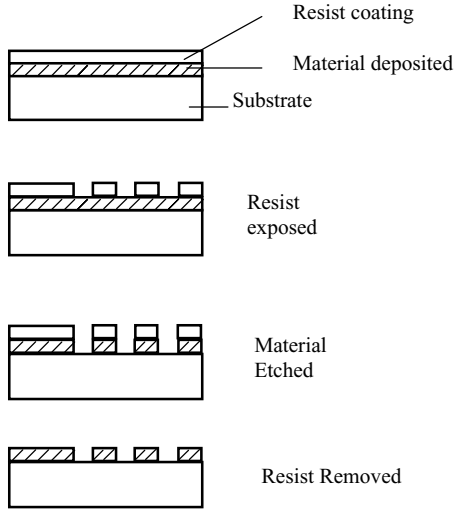

Figure 15. Subtractive pattern transfer process.

in a direction perpendicular to the substrate. This way, the etching is anisotropic or only in the vertical direction thereby eliminating undercutting effects. This process is used today, almost exclusively, for the patterning of most layers, including metals, in memory and logic circuit production with a few exceptions where lift-off is still used.

It should be mentioned that for additive processes positive resists are generally used because it is not possible to obtain the required undercut profiles from negative resists due to electron beam scattering effects, as seen in Figure 13, which force negative resists to develop sloping profiles, opposite to undercut. In subtractive processes, however, any resist can be used. In most subtractive cases the resist profile is replicated on the substrate after etching since the resist is also etched during substrate etching.

The etching of silicon, silicon oxides or silicon nitrides is done with gas mixtures that contain fluorine as the active gas while metals such as aluminum or chromium require chlorine gas for etching. Reactive ion etching systems use, in general, two parallel plates with the top plate grounded and the bottom plate, on to which the samples or silicon wafers to be etched are placed, connected to the RF power source, typically set at 13.5 MHz. Since the resist is also etched during the process, the plasma parameters, such as power, pressure, gas flow and gas composition, have to be optimized in order to increase the etching selectivity between resist and other materials.

It has been found that acrylic-type polymers, such as PMMA or its copolymers, are not very stable in the plasma and, therefore not very useful in RIE transfer processes, while phenolic-type polymers of which most AZ-type photo-resists are made, are much more stable and more widely used. For this reason and because phenolic resins can resist higher temperatures than acrylic polymers, all new resists, including the new, acid-catalyzed ones use as their base resin phenolic or aromatic polymers. Also, the choice between positive or negative resists is independent of the RIE process, as long as both types are made with aromatic polymers, and depends only on the density of the circuit pattern. This is especially true with electron beam lithography where the pattern polarity (and the resist) is chosen to minimize the beam writing time.

The resolution of the new, very sensitive acid-catalyzed resists does not approach that of PMMA. At this moment, it can only resolve line widths in periodic patterns of about 0.2 μm in 0.4-μm thick layers. While intensive investigation is been performed in many labs, PMMA is still in use for sub-100 nm structures.

5. APPLICATIONS IN NANOTECHNOLOGY

5.1. Mask Making

5.1.1. IC Fabrication Mask

As microelectronics continues to advance, the field has been extended from micrometer to nanometer scale, hence the development of nanotechnology and nanoelectronics. However, nanoscale mask making remains the key technique in nanoelectronics technology, as it has been in microelectronics technology. Due to its inherently high spatial resolution (less than 1 nm) and wide process margins, EBL is still the technological choice for mask making.

The most popular and well-established mask making system is the MEBES [41]. The MEBES uses a focused Gaussian spot to write a pattern in stripes while moving the stage continuously. The beam deflection is primarily in one direction, perpendicular to the motion of the stage. The MEBES is designed for high-throughput mask making, with a minimum feature size of 0.25 m.

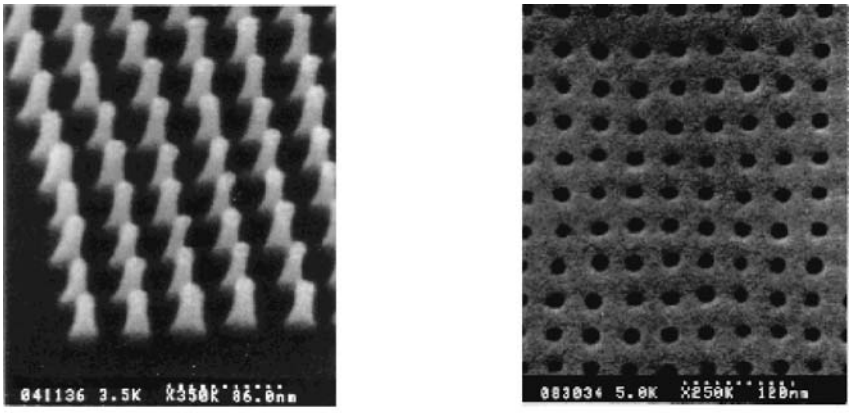

Figure 16. (a) Imprint mold with 10 nm diameter pillars (b) 10 nm diameter holes imprinted in PMMA (Stephen Y. Chou, Princeton).

The EBES4 mask making system [42] is another system using a Gaussian spot. In this system the coarse/fine DAC beam placement is augmented with an extra (third) deflection stage, and the mask plate is moved continuously, using the laser stage controller to provide continuous correction to the stage position. The EBES4 mask making system has a spot size of 0.12 um, uniformity to 50 nm (3), stitching error of 40 nm, and repeatability of 30 nm over a 6 in. reticle.

5.1.2. Nanoimprint Mask

Nanoimprint lithography [43] patterns a resist by deforming the resist shape through embossing (with a mold), rather than by altering resist chemical structures through radiation (with particle beams). After imprinting the resist, an anisotropic etching is used to remove the residue resist in the compressed area to expose the substrate underneath. It is a major breakthrough in nanotechnology because it can produce sub-10 nm feature size over a large area with a high throughput and low cost.

One of the key elements for nanoimprint lithography is the mold, which relies on EBL technology to be produced. Figures 16 shows an imprint mold with 10 nm diameter pillars and the 10 nm diameter holes imprinted in PMMA material.

5.1.3. X-ray Lithography Mask

X-ray lithography's (XRL) penetrative power and scatterings free of X-rays are two primary reasons for its popularity in nanotechnology and nanofabrication. But, the mask fabrication has been the most difficult challenge to XRL. The XRL mask consists of a thin layer (200–250 nm) of X-ray absorbent material (e.g. Au and W), supported

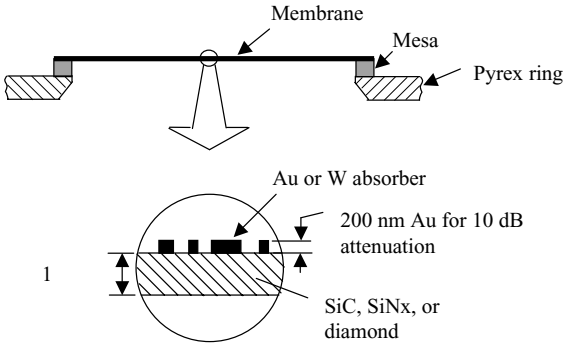

Figure 17. An x-ray mask configuration suitable for a 10–dB attenuation at the wavelength of 1.32 nm (Henry I. Smith and M. L. Schattenburg, MIT).

on a thin membrane (~1 μm) that is 20–30 mm in diameter. Figure 17 shows a mask configuration suitable for a 10-dB attenuation at the 1.32 nm radiation. The primary concern for the mask is distortion, which can be introduced by the following four sources: the original mask patterning; the mask frames; radiation damage; or absorber stress. To have a reasonable yield of the desired nanostructure, mask distortion at any point in a pattern should not exceed 1/5 to 1/10 of the minimum feature size. For a 10 nm feature, the distortion should be no more than a couple of nanometers.

Many techniques, such as e-beam lithography, photolithography, holographic lithography, X-ray lithography, and ion-beam lithography, have been developed to make XRL masks. But, e-beam lithography is the most frequently used method. Either additive or subtractive process has been used for pattern formation on the mask.

Examples of x-ray mask fabrication schemes for an Au additive process are shown in Figure 18. The process involves plating x-ray absorber on the resist-patterned membrane. It includes deposition of membrane film on a silicon wafer, back-etching the silicon to the membrane film, glass frame attachment, deposition of chrome for plating base, resist coating, pattern formation by electron beam lithography, Au plating (additive process), and finally resist removal. Figure 19 is an actual X-ray mask with 75 nm features fabricated by EBL.

5.2. Direct Writing

5.2.1. Self-Assembly

Carbon nanotubes (NTs) [44] have opened a promising path in nanotechnology. They provide insulating, semiconducting or truly conducting nanoscale wires for electronic applications. Devices such as a junction [45–47] and a field-effect transistor [48–51] have been demonstrated. But, up to now, all the demonstrated NT electrical devices have been fabricated either by randomly depositing NTs on a multi-electrode array or by patterning contacts onto randomly deposited NTs, after their observation.

K. H. Choi *et al.* [52] demonstrated a method for achieving controlled fabrication with the help of the EBL. This method is based on the electrostatic anchoring of

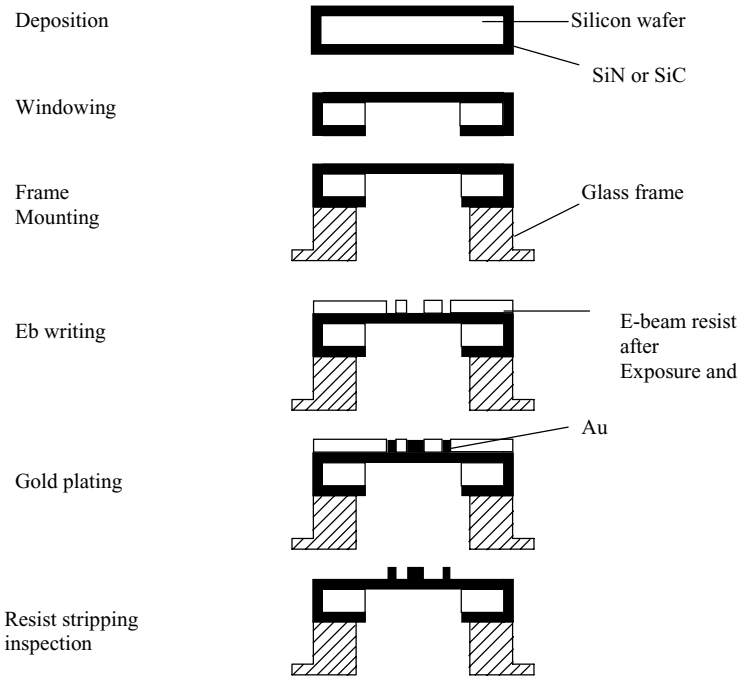

Figure 18. A gold additive process for x-ray mask fabrication.

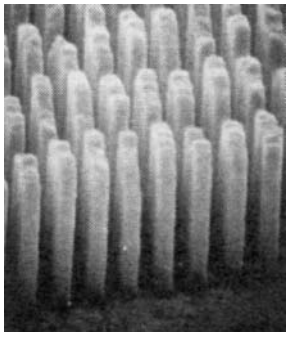

Figure 19. 75 nm features of plated gold absorber on an X-ray membrane.

surfactant covered NTs onto amino-silane functionalized surfaces [53]: first, a reactive amino-silane template is prepared using chemical vapour deposition of silane molecules through a PMMA mask patterned by conventional electron-beam lithography. Surfactant covered NTs are then selectively deposited onto the template. Finally, the PMMA mask is lifted-off, leaving the tubes on the template. Figure 20 shows AFM images of NTs onto the patterned silane monolayer. The typical thickness of the NTs of (a) (measured relative to the silane surface) is 1.6 ± 0.2 nm.

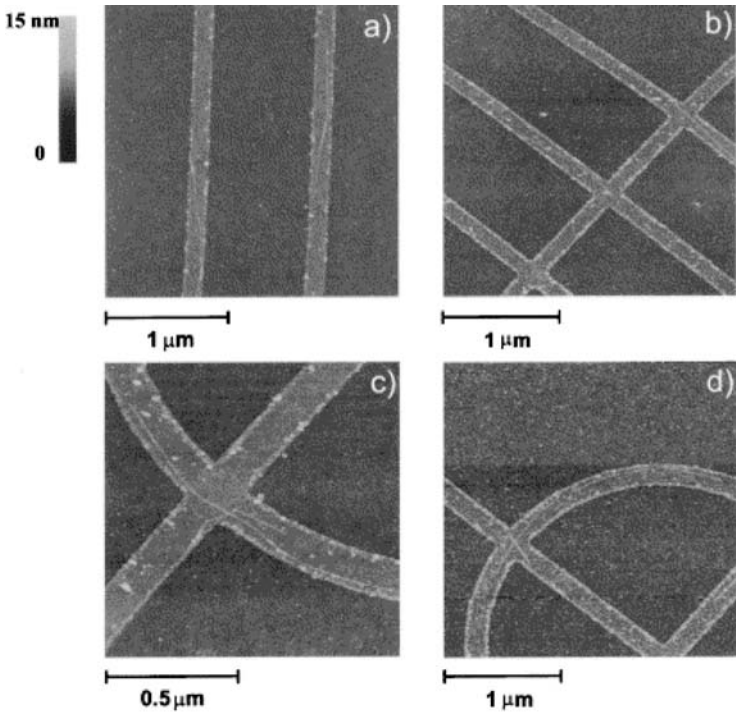

Figure 20. NTs onto the patterned silane monolayer. The silane stripes appear brighter than the bare silica surface. The NTs appear brighter than the silane stripes onto which they are adsorbed (K. H. Choi *et al.*, 2000).

Similarly, patterned amine-functionalized self-assembled monolayers have potential as a template for the deposition and patterning of a wide variety of materials on silicon surfaces, including biomolecules. C. K. Harnett *et al.* [54] obtained results for low-energy electron-beam patterning of 2-aminopropyltriethoxysilane and (aminoethylaminomethyl) phenethyltrimethoxysilane self-assembled monolayers on silicon substrates. They demonstrated that, on the ultrathin (1–2 nm) monolayers, lower electron beam energies (<5 keV) produce higher resolution patterns than high-energy beams. At 1 keV, a dose of 40 $\mu C/cm^2$ is required to make the patterns observable by lateral force microscopy. Features as small as 80 nm were exposed at 2 keV on these monolayers. After exposure, palladium colloids and aldehyde- and protein-coated polystyrene fluorescent spheres adhered only to unexposed areas of the monolayers.

5.2.2. Nanoscale Device Fabrication

The steps taken to produce a nanoscale device by EBL are shown in Figure 21: the sample is covered with a thin layer of PMMA, then the desired structure or pattern is exposed with a certain dose of electrons. The exposed PMMA changes its solubility

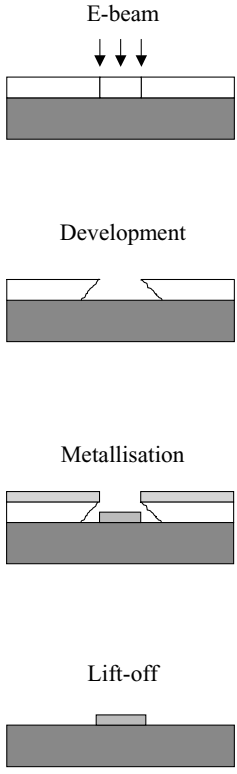

Figure 21. EBL steps for fabricating nanoscale devices.

towards certain chemicals. This can be used to produce a trench in the thin layer. If one wants to produce a metallic structure, a metal film is evaporated onto the sample and after dissolving the unexposed PMMA with its cover (lift-off) the desired metallic nanostructure remains on the substrate.

Until recently, the EBL system was used almost exclusively for fabricating research and prototype nanoelectronic devices. It is still the only tool used for this kind of device scale since a lithography system for mass production is not available for deep nanometer features [55–57]. Devices fabricated by using EBL include quantum dots, single electron transistors [58], nanotube transistors [59], and other nanoscale structures.

The following four examples of nanoscale structures are fabricated by using EBL. Figure 22 is a pattern for "Binary position-modulated sub-wavelength grating (BPMSG)" [60] fabricated using a "lift-off" process. BPMSG is a very important building block for many micro scale optical instruments such as spectrometers and multiplexors.

In Figure 23, the hexagon array was written with the beam making a single pass over each line. First, the beam moved back and forth across the entire structure writing the non-vertical lines. Then, each short vertical line was written to complete the pattern.

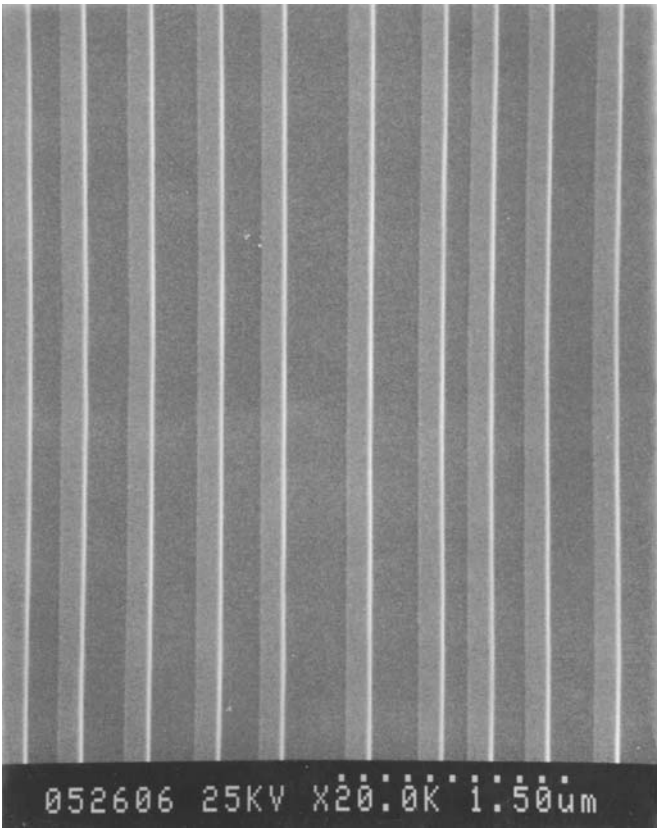

Figure 22. EBL generated 150 nm chromium lines with variable spaces ranging from 150 nm to 300 nm on a silicon substrate. The thickness of the lines is about 100 nm. [Zhou, 1993].

Figures 24–25 were fabricated at the Nanoscale Science Laboratory of the University of Cambridge headed by Professor Mark Welland [61]. Figure 24 is a field-emitting device fabricated on silicon. Its feature size is in the 100 nm regime. Source, drain and gate are made from tungsten.

Figure 25 shows a line of 5 nm wide written into PMMA. This line has a homogeneous width over more than 100 nm and is an example of the smallest features that can be produced with electron beam lithography.

5.2.3. Electron Beam Processing

Another important application of electron beams is their use as energy carriers for the local heating of a work point in a vacuum. Electron beams are specially used to carry high power densities and to generate a steep temperature rise on the work point. Furthermore, the energy input at the work point can be accurately controlled

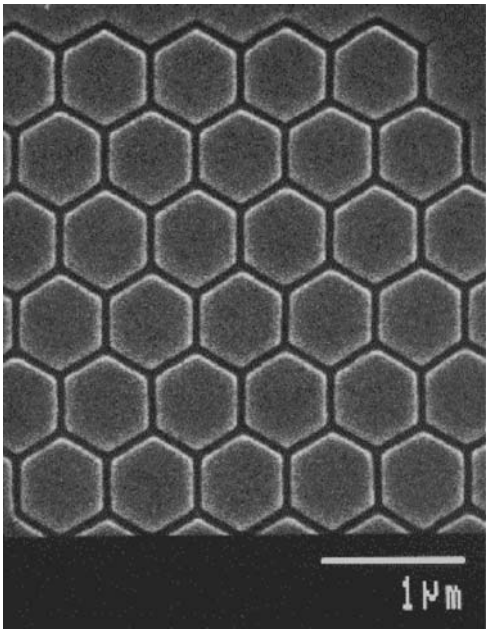

Figure 23. EBL generated Hexagons. Copyright (c) 1996 JC Nabity Lithography Systems.

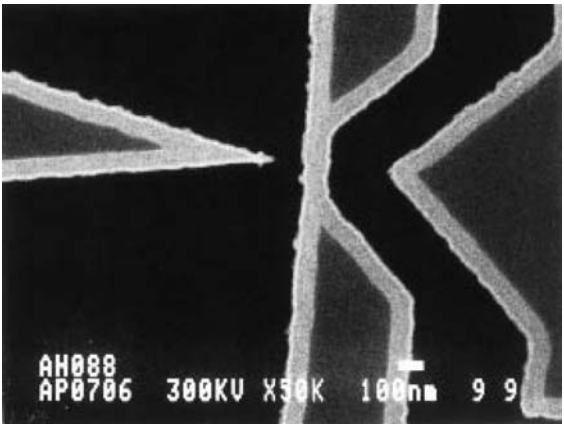

Figure 24. A field-emitting device fabricated on silicon using EBL.

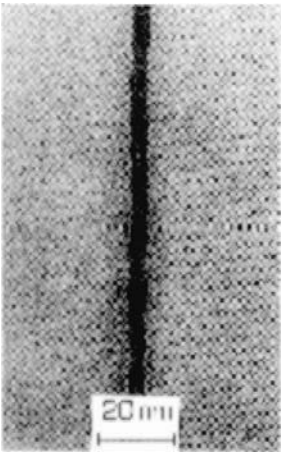

Figure 25. A line of 5 nm in width written into PMMA by EBL.

with respect to time and space. With such desirable characteristics, electron beam processing has been widely used in semiconductor manufacturing for the last three decades.

More recently, patterning of porous silicon (PS) at the nanometer length scale has been obtained by electron-beam-induced carbon masking [62]. This technique is able to locally modify or mask the Si substrate before the PS formation. It provides great possibilities in the field of micromachining [63] and photonics [64–65].

On the other hand, direct electron-beam irradiation of semiconductor surfaces has been attempted in recent years to remove H passivation [66] or to favor O desorption [67]. In many cases, it has been demonstrated that, as a consequence for this treatment(s), the surface shows a selective reactivity to subsequent treatments. The same effect, even larger as a consequence for the higher reactivity, can be expected for nanoporous silicon (NPS). This direct electron-beam treatment on PS opens the possibility of defining nanometer-sized structures on a nanosized material.

The availability of EBL apparatus allows for the structuring of several semiconducting and metallic materials down to few tens of nm. For these reasons, electron irradiation of submicrometric areas of PS can have interesting applications in micromachining and could allow for the realization of two- or three-dimensional photonic structures.

6. SUMMARY AND FUTURE PERSPECTIVES

One of the methods to create functional materials, devices, and systems through the control of matter at the atomic or molecular level is the top-down miniaturization.

The top down approach downsizes things from large-scale structures into small-scale structures. It is the major method used for the microelectronics development. As the microelectronics technology continues to advance, it has been extended from

micrometer to nanometer scale, hence the "nanotechnology" or "nanofabrication". Using nanotechnology, the narrowest line pattern on mass produced semiconductor devices is now approaching the 50-nanometer level. In research labs, horizontal dimensions of the device feature sizes have been further scaled down from 130 nanometers to 6 nanometers and its vertical dimensions have been reduced to less than 1.5 nanometers or a couple of atoms.

The heart of the top-down approach of miniaturization processing is the nanolithography technique. Among many techniques of nanolithography, the EBL technique is, at least for now, the best choice for ultimate nanoscale structures due to its ability to precisely focus and control electron beams onto various substrates, and therefore, create virtually any kind of nanostructures. It has been demonstrated that electron beams can be focused down to less than 1 nm. This will extend the resolution of EBL to the sub-nanometer region provided that appropriate resistant material is available.

However, parallel writing schemes of EBL have to be developed so that higher throughput can be achieved.

REFERENCES

1. Bruce Doris, Meikei Ieong, Thomas Kanarsky, Ying Zhang, Ronnen A. Roy, Omer Dokumaci, Zhibin Ren, Fen-Fen Jamin, Leathen Shi, Wesley Natzle, Hsiang-Jen Huang, Joseph Mezzapelle, Anda Mocuta, Sherry Womack, Michael Gribelyuk, Erin C. Jones, Robert J. Miller, H-S Philip Wong, and Wilfried Haensch, IEDM Tech. Dig. (2002), pp. 267–270.
2. Timp, G., Bude, J., Bourdelle, K. K., Garno, J., Ghetti, A., Gossmann, H., Green, M., Forsyth, G., Kim, Y., Kleiman, R., Klemens, F., Kornblit, A., Lochstampfor, C., Mansfield, W., Moccio, S., Sorsch, T., Tennant, D. M., Timp, W., and Tung, R., IEDM Tech. Dig. (1999).
3. Smith, K. C. A., and Oatley, C. W., Br. J. Appl. Phys., 6, 391 (1955).
4. Broers, A. N., in *Proceedings of the First International Conference on Electron and Ion Beam Technology* (R. Bakish, ed.) Wiley, New York, p. 181, 1964.
5. Broers, A. N., Molten, W. W., Cuomo, J. J., and Wittels, N. D., Appl. Phys. Lett., 29, 596 (1976).
6. Umbach, C. P, Washburn, S., Laibowitz, R. B., and Webb, R. A., Phys. Rev. B, 30, 4048 (1984).
7. Muray, A., Scheinfein, M., Isaacson, M., and Adesida, I., J. Vac. Sci. Technol. B, 3, 367 (1985).
8. Y. Yau, R. F. W. Pease, A. Iranmanesh, and K. Polasko, J. Vac. Sci. Technol., 19, 1048 (1981).
9. Child, D. C., *Phys. Rev.*, 32, p. 492 (1911).
10. Lafferty, J. M. Boride cathode. *J. Appl. Phys.* 22(3), pp. 299–309 (1951).
11. Morley, J. R., *Proc. Third Symp. Electron Beam Tech.* p. 26 (1961).
12. Sayegh, G., Dumonte, P., Theoretical and experimental techniques for design of electron beam welding guns, effect of welding conditions on electron beam characteristics. In Salva, R. M. *Third electron Beam Processing Seminar*, Stratford-upon-Avon, England, 1974. Dayton, Ohio: Universal Technology (1974), pp. 3a1–3a87.
13. T. H. P. Chang, "Proximity effect in electron beam lithography," *J. Vac. Sci. Technol.* **12**, 1271–1275 (1975).
14. D. F. Kyser and N. S. Viswanathan, "Monte Carlo simulation of spatially distributed beams in electron-beam lithography," *J. Vac. Sci. Technol.* **12**(6), 1305–1308 (1975).
15. K. K. Christenson, R. G. Viswanathan, and F. J. Hohn, "X-ray mask fogging by electrons backscattered beneath the membrane," *J. Vac. Sci. Technol.* **B8**(6), 1618–1623 (1990).
16. J. Ingino, G. Owen, C. N. Berglund, R. Browning, R. F. W. Pease, "Workpiece charging in electron beam lithography," J. Vac. Sci. Technol. **B12** (3) 1367 (1994).
17. Gold etch solution type TFA from Transene Co., Rowley MA.
18. Chrome etch type CR-14 from Cyantek Corp., 3055 Osgood Ct., Fremont CA 94538.
19. Broers, A. N., J. Electrochem. Sec., 128, 166 (1981).
20. D. W. Keith, R. J. Soave, M. J. Rooks, "Free-standing gratings and lenses for atom optics," J. Vac. Sci. Technol. **B9** (6) 2846 (1991).

21. W. C. B. Peatman, P. A. D. Wood, D. Porterfield, T. W. Crowe, M. J. Rooks, "Quarter-micrometer GaAs Schottky barrier diode with high video responsivity at 118 m," Appl. Phys. Lett. **61** 294 (1992).
22. R. C. Tiberio, G. A. Porkolab, M. J. Rooks, E. D. Wolf, R. J. Lang, A. D. G. Hall, "Facetless Bragg reflector surface-emitting AlGaAs/GaAs lasers fabricated by electron-beam lithography and chemically assisted ion-beam etching", J. Vac. Sci. Technol. **B9** 2842 (1991).
23. T. Tada, "Highly sensitive positive electron resists consisting of halogenated alkyl -chloroacrylate series polymer materials," J. Electrochem. Soc. **130** 912 (1983).
24. K. Nakamura, S. L. Shy, C. C. Tuo, C. C. Huang, "Critical dimension control of poly-butene-sulfone resist in electron beam lithography," Jpn. J. Appl. Phys. **33**, 6989 (1994).
25. M. Widat-alla, A. Wong, D. Dameron, C. Fu, "Submicron e-beam process control," Semiconductor International (May 1988), p. 252.
26. Nippon Zeon is represented in the US by Nagase California Corp., 710 Lakeway, Suite 135, Sunnyvale, CA 94086. 408-773-0700.
27. E. Reichmanis, L. F. Thompson, "Polymer materials for microlithography," in *Annual Review of Materials Science*, v.17, R. A. Huggins, J. A. Giordmaine, J. B. Wachtman Jr., eds. (Annual Reviews, Palo Alto, 1987) p.238.
28. Mead Chemical Co., 10750 County Rd. 2000, PO Box 748, Rolla, MO 65401. 314-364-8844.
29. C. G. Willson, "Organic Resist Materials", and L. F. Thompson, "Resist Processing", in *Introduction to Microlithography, Second Edition,* L. F. Thompson, C. G. Willson, M. J. Bowden, eds. (American Chemical Society, Washington DC, 1994).
30. Shipley Inc., 455 Forest St., Marlboro, MA 01752. 800-343-3013.
31. T. Yoshimura, Y. Nakayama, S. Okazaki, "Acid-diffusion effect on nanofabrication in chemical amplification resist," J. Vac. Sci. Technol. **B10**(6) 2615 (1992).
32. E. A. Dobisz, C. R. K. Marrian, "Sub-30 nm lithography in a negative electron beam resist with a vacuum scanning tunneling microscope," Appl. Phys. Lett. **58**(22) 2526 (1991).
33. A. Claßen, S. Kuhn, J. Straka, A. Forchel, "High voltage electron beam lithography of the resolution limits of SAL601 negative resist," Microelectronic Engineering **17** 21 (1992).
34. W. Moreau, C. H. Ting, "High sensitivity positive electron resisit," US Patent 3934057, 1976.
35. S. Mackie, S. P. Beaumont, Solid State Technology **28** 117 (1985).
36. R. E. Howard, E. L. Hu, L. D. Jackel, "Multilevel resist for lithography below 100 nm," IEEE Trans. Electron. Dev. **ED-28**(11) 1378 (1981).
37. R. E. Howard, D. E. Prober, "Nanometer-scale fabrication techniques," in *VLSI Electronics: Microstructure Science* vol. 5 (Academic Press, New York, 1982).
38. R. C. Tiberio, J. M. Limber, G. J. Galvin, E. D. Wolf, "Electron beam lithography and resist processing for the fabrication of T-gate structures," Proc. SPIE **1089**, 124 (1989).
39. M. Hatzakis, C. H. Ting, and N. Viswanathan, in *Proceedings of the Symposium on Electron and Ion Beam Science and Technol.*, ECS Inc., Princeton, NJ, 542–579 (1974).
40. A. R. Neureuther, D. F. Kyser, K. Murata, and C. H. Ting, in *Proceedings of the Symposium on Electron and Ion Beam Science and Technol.*, ECS Inc., Princeton, NJ, 265–275 (1978).
41. M. Gesley, F. Abboud, D. Colby, F. Raymond, S. Watson, "Electron beam column developments for submicron- and nanolithography," Jpn. J. Appl. Phys. **32** 5993 (1993).
42. Lepton Inc., Murray Hill NJ 07974, 908-771-9490.
43. Stephen Y. Chou, Peter R. Krauss, and Preston J. Renstrom, J. Vac. Sci. Technol. B 14 (1996) 4129.
44. S. Iijima. *Nature* **354** (1991), p. 56.
45. R. D. Antonov and A. T. Johnson. *Phys. Rev. Lett.* **83** (1999), p. 3274.
46. Z. Yao, H. W. C. Postma, L. Balents and C. Dekker. *Nature* **402** (1999), p. 273.
47. M. S. Fuhrer, J. Nygard, L. Shih, M. Forero, Y. G. Yoon, M. S. C. Mazzoni, H. J. Choi, J. Ihm, S. G. Louie, A. Zettl and P. L. McEuen. *Science* **288** (2000), p. 494.
48. S. J. Tans, A. R. M. Vershueren and C. Dekker. *Nature* **39** (1998), p. 49.
49. R. Martel, T. Schmidt, T. Hertel and P. Avouris. *Appl. Phys. Lett.* **73** (1998), p. 2447.
50. L. Roschier, J. Penttilae, M. Martin, P. Hakonen, M. Paalanen, U. Tapper, E. Kauppinen, C. Journet and P. Bernier. *Appl. Phys. Lett.* **75** (1999), p. 728.
51. H. T. Soh, A. F. Morpurgo, J. Kong, C. M. Marcus, C. F. Quate and H. Dai. *Appl. Phys. Lett.* **75** (1999), p. 627.
52. K. H. Choi, J. P. Bourgoin, S. Auvray, D. Esteve, G. S. Duesberg, S. Roth, and M. Burghard, Surface Science, 462 (2000), pp. 195–202.
53. M. Burghard, G. S. Duesberg, G. Philipp, J. Muster and S. Roth. *Adv. Mater.* **10** (1998), p. 584.
54. C. K. Harnett, K. M. Satyalakshmi, and H. G. Craighead, App. Phys. Lett., 76 (2000), pp. 2466–2468.

55. Beaumont S. P., Bower P. G., Tamamura T. and Wilkinson C. D. W., Appl. Pliys. Lett., 38 (1981) 436.
56. Craighead H. G., Howard R. E., Jackel L. D, and Mankiewich P. M., Appl. Phys. Lett., 42 (1983) 38.
57. Ochiai Y., Baba M., Watanabe H. and Matsui S., Jpn. J. Appl. Phvs., 30 (1991) 3266.
58. Claes Thelander, Martin H. Magnusson, Knut Deppert, Lars Samuelson, Per Rugaard Poulsen, Jesper Nygård, and Jørn Borggreen, Appl. Phys. Lett.79 (2001) pp 2106–2108.
59. S. J. Tans *et al.*, Nature, 7 May 1998.
60. Zhou, Z. J., Ph.D. Thesis, Georgia Institute of Technology (1993).
61. http://www-g.eng.cam.ac.uk/nano/emlitho.htm last visited on August 30, 2003.
62. T. Djenizian, L. Santinacci, and P. Schmuki, Appl. Phys. Lett. **78**, 2940 (2001).
63. W. Lang, P. Steiner, and H. Sandmaier, Sens. Actuators A **51**, 31 (1995).
64. P. Ferrand, D. Loi, and R. Romestain, Appl. Phys. Lett. **79**, 3017 (2001).
65. A. M. Rossi, G. Amato, V. Camarchia, L. Boarino, and S. Borini., Appl. Phys. Lett. **78**, 3003 (2001).
66. F. Y. C. Huy, G. Eres, and D. C. Joy, Appl. Phys. Lett. **72**, 341 (1998).
67. T. Yasuda, D. S. Hwang, J. W. Park, K. Ikuta, S. Yamasaki, and K. Tanaka, Appl. Phys. Lett. **74**, 653 (1999).